CHEMICAL ENGINEERING TRANSACTIONS
VOL. 43, 2015
A publication of AIDIC
The Italian Association of Chemical Engineering
Online at www.aidic.it/cet
Chief Editors: Sauro Pierucci, Jiří J. Klemeš

ISBN 978-88-95608-34-1; **ISSN** 2283-9216
DOI: 10.3303/CET1543178

How Does Radial Convection Influence the Performance of Membrane Module for Gas Separation Processes?

Maria Anna Murmura*[a], Luca Turchetti[b], Rosaria Augelletti[a], Maria Cristina Annesini[a], Stefano Cerbelli[a]

[a]Dipartimento di Ingegneria Chimica Materiali Ambiente, Sapienza Università di Roma, Via Eudossiana 18 – 00184 Rome (Italy)
[b]ENEA, Italian Agency for New Technologies, Energy and Environment Technical Unit for Renewable Energy Sources UTRINN, Via Anguillarese 301 – 00123 Rome (Italy)
mariaanna.murmura@uniroma1.it

A two-dimensional axial-symmetric isothermal model, based on full coupling between mass and momentum transport, has been developed to describe the separation of a binary gaseous mixture in a packed bed membrane module. Steady-state conditions have been studied. The gaseous mixture to be separated enters an annular gap between two co-axial cylinders. The inner wall of the outer cylinder is impermeable to both components, whereas a membrane, with infinite selectivity towards one of the components, is supported onto the outer wall of the inner cylinder. A radial flux of the permeating components is therefore present. The main focus was on the determination of the influence of radial convection on the performance of the separator, which has been analysed in terms of three dimensionless groups. Different transport regimes could be identified, corresponding to different values of the dimensionless groups. The impact of radial convection has been assessed by comparing model predictions with those of a fully uncoupled one-dimensional model. A discrepancy up to 20% of the recovery has been observed in industrially relevant ranges of the parameters.

1. Introduction

Integration of reaction and separation in a single unit may bring to significant increases in the efficiency of many chemical processes (Giaconia et al., 2013). Membrane reactors have been studied experimentally (Santucci et al., 2011) and models have been widely presented in literature. In most models the radial component of velocity is neglected, without a quantitative analysis of the errors caused by this assumption. This is found for example in Godini et al. (2014), who studied ethylene production, and in Jin et al. (2000), who studied partial oxidation of methane. As pointed out by Nekhamkina and Sheintuch (2014), these errors may concern the evaluation of both the velocity profiles in the reactor and the total recovery of the permeating component. A more accurate model may therefore be necessary to understand the system's behaviour, and to carry out an efficient optimization of reactor design. Studies in this direction will become increasingly important as higher permeance membranes are developed.
In the present work a simple gas separation is studied as a basis for membrane reactor modelling. A two-dimensional model is developed in which the coupling between mass and momentum transport is considered. The results obtained are compared with a simpler model, where fluid-dynamics are decoupled from transport of the permeating species. Model predictions are compared to determine the cases in which the simplified model describes the behaviour of the reactor accurately enough.

2. Model Development

A 2D axial-symmetric isothermal steady-state model has been developed to describe the separation of a binary gaseous mixture. The shell and tube configuration described above is often found when dealing with

Please cite this article as: Murmura M.A., Turchetti L., Augelletti R., Annesini M.C., Cerbelli S., 2015, How does radial convection influence the performance of membrane module for gas separation processes?, Chemical Engineering Transactions, 43, 1063-1068
DOI: 10.3303/CET1543178

hydrogen permeable membranes, consisting of a thin Pd layer on a ceramic support. In the present case the separation of a hydrogen/methane mixture is considered. The two components will be referred to with the subscripts *h* and *m*, respectively. The symbol ∇ will represent the two-dimensional gradient operator in the radial and axial coordinates.

2.1 Model Equations

Gas separation is usually carried out in empty tube modules, in which the motion of the gas may be described by the Navier-Stokes equation. Since the objective of this work is to set the basis for membrane reactor modelling, the presence of granular packing has been considered, and motion of the fluid has been described through Darcy's equation:

$$\mathrm{v} = -\frac{\kappa}{\mu}\nabla P \tag{1}$$

where **v** is the mass average gas velocity, κ is the bed permeability, μ is the viscosity of the gaseous mixture, and *P* the pressure. At steady state conditions, the overall mass balance is:

$$\nabla \cdot (\rho \mathrm{v}) = 0 \tag{2}$$

where ρ is the mass density of the mixture.
By substituting Eq(2) into Eq(1), and if the bed permeability and gas viscosity are considered to be constant throughout the module, the continuity equation may be re-written as:

$$\nabla \cdot (\rho \nabla P) = 0 \tag{3}$$

If ideal behaviour is assumed for the gaseous mixture, its density may be expressed as:

$$\rho = f(\omega_h)\frac{P}{RT}\text{, with } \frac{1}{f(\omega_h)} = \frac{\omega_h}{W_h} + \frac{1-\omega_h}{W_m} \tag{4}$$

where ω_i and W_i indicate the mass fraction and the molecular weight, respectively, of the *i-th* component. Substituting Eq.(4) into Eq.(3) gives:

$$\nabla \cdot (fP\nabla P) = 0 \tag{5}$$

Eq(5) highlights the fact that even in isothermal conditions, the pressure distribution within the packed bed is influenced by gas composition through the factor *f*. The pressure distribution, in turn, determines the velocity profile through Darcy's equation.
The mass balance equation for the permeating component has been written in terms of mass fraction, considering convective and dispersive mechanisms in both the radial and the axial directions:

$$\frac{1}{RT}\nabla \cdot \left(-\frac{\kappa}{\mu} fP\omega_h \nabla P - fP\mathbb{D} \cdot \nabla \omega_h\right) = 0\text{; where } \mathbb{D} = \begin{pmatrix} \mathcal{D}_{rr} & 0 \\ 0 & \mathcal{D}_{zz} \end{pmatrix} \tag{6}$$

is the effective dispersion tensor, generally non-isotropic. Dispersion coefficients account for two phenomena: molecular diffusion and convection due to the movement of fluid particles through the intricate geometry of the packed bed. Obviously, in a two-component system the continuity equation, Eq(5), and mass balance of one component, Eq(6), fully define the problem.

2.2 Boundary Conditions

The continuity and mass balance equations presented above have been solved by assuming the membrane on the inner wall of the annular section is permeable only to component *h*. Hydrogen permeation through Pd membranes involves the following steps:

1. Molecular transport from the bulk of the gas to the gas layer adjacent to the membrane surface;
2. Dissociative adsorption of hydrogen onto the membrane surface;
3. Transition of atomic H from the surface to the bulk;
4. Atomic diffusion through the bulk;
5. Transition from the bulk to the surface of the permeate side;
6. Recombinative desorption from the surface;

7. Gas transport away from the surface to the bulk of the gas.

For clean membranes, operating at temperatures above 300°C and with a Pd layer thickness down to 1μm, it has been found that diffusion of H atoms through the bulk of the membrane is rate-limiting (Ward and Dao, 1999). In these conditions Sievert's law applies, and hydrogen flux through the membrane is evaluated as:

$$J_h = \frac{\phi}{\delta}\left(\sqrt{P_h} - \sqrt{P_h^p}\right) = \mathbb{P}_m\left(\sqrt{P_h} - \sqrt{P_h^p}\right) \tag{8}$$

where ϕ is the intrinsic permeability of the membrane, δ is its thickness, $\mathbb{P}_m$ is the overall permeability, P_h is the partial pressure of hydrogen in the retentate side, and P_h^p is the partial pressure of hydrogen in the permeate side. In the development of this model, P_h^p has been always assumed to be equal to zero.
Boundary conditions are therefore written as:

$$\omega_i|_{z=0} = \omega_i^0 \quad ; \quad \mathbf{v}|_{z=0} = v_z^0 \tag{9}$$

$$\left.\frac{\partial \omega_i}{\partial z}\right|_{z=L} = 0 \quad ; \quad P|_{z=L} = P_L \tag{10}$$

$$\nabla\omega_i \cdot \mathbf{n}|_{r=R_2} = 0 \quad ; \quad \nabla \mathrm{P} \cdot \mathbf{n}|_{r=R_2} = 0 \tag{11}$$

$$\left(-\frac{\kappa}{\mu}\omega_h f P \nabla P - f P \mathbb{D} \cdot \nabla \omega_h\right) \cdot \mathbf{n}\Big|_{r=R_1} = RT\mathbb{P}_m\left(\sqrt{\omega_h f P / W_h}\right) \tag{12}$$

$$\left(-\frac{\kappa}{\mu} f P \nabla P\right) \cdot \mathbf{n}\Big|_{r=R_1} = RT\mathbb{P}_m\left(\sqrt{\omega_h f P / W_h}\right) \tag{13}$$

Where **n** is a unit vector normal to the cylindrical surface and directed inwards.

2.3 Dimensionless Formulation

The equations reported above may be re-written in terms of dimensionless variables. This allows the identification of characteristic groups, which aid in the comprehension of the mechanisms governing the system performance. The following dimensionless variables have been chosen:

$$\tilde{\mathbf{v}} = \frac{\mathbf{v}}{v_z^0}$$

$$\tilde{r} = \frac{r}{R_1} \quad ; \quad \tilde{z} = \frac{z}{R_1}$$

$$\tilde{f} = \frac{f}{W_h}$$

$$\tilde{P} = \frac{P}{P_U} \quad \text{with} \quad P_U = \frac{\mu v_z^0 R_1}{\kappa}$$

With such substitutions, the continuity and mass balance equations become:

$$\tilde{\nabla} \cdot \left(\tilde{f}\tilde{P}\tilde{\nabla}\tilde{P}\right) = 0 \tag{14}$$

$$\tilde{\nabla} \cdot \left(\tilde{f}\tilde{P}\omega_h\tilde{\nabla}\tilde{P} - \frac{1}{Pe}\tilde{f}\tilde{P}\tilde{\mathbb{D}} \cdot \tilde{\nabla}\omega_h\right) = 0 \tag{15}$$

where $\tilde{\nabla}$ is the dimensionless operator and the Peclet number, *Pe*, represents the ratio between the characteristic times of diffusion and convection and is defined as:

$$Pe = \frac{v_z^0 R_1}{\mathcal{D}} \tag{16}$$

Boundary conditions in the dimensionless form become:

$$\omega_i|_{z=0} = \omega_i^0 \quad ; \quad \tilde{\mathbf{v}}|_{z=0} = 1 \tag{17}$$

$$\left.\frac{\partial \omega_i}{\partial \tilde{z}}\right|_{\tilde{z}=L/R_1} = 0 \quad ; \quad \tilde{P}\Big|_{\tilde{z}=L/R_1} = \alpha \quad \text{with } \alpha = \frac{P_L}{P_U} = P_L \frac{\kappa}{\mu v_z^0 R_1} \tag{18}$$

$$\widetilde{\nabla}\omega_i \cdot \mathbf{n}\Big|_{\tilde{r}=R_2/R_1} = 0 \quad ; \quad \widetilde{\nabla}\mathrm{P} \cdot \mathbf{n}\Big|_{\tilde{r}=R_2/R_1} = 0 \tag{19}$$

$$\left(\omega_h \widetilde{\nabla}\tilde{P} + \frac{1}{Pe}\widetilde{\mathbb{D}} \cdot \widetilde{\nabla}\omega_h\right) \cdot \mathbf{n}\Big|_{\tilde{r}=1} = -\gamma \sqrt{\frac{\omega_h}{\tilde{f}\tilde{P}}} \quad \text{with } \gamma = \frac{\mathbb{P}_m}{W_h} RT \left(\frac{\mu R_1}{\kappa}\right)^{-1/2} (v_z^0)^{-3/2} \tag{20}$$

$$\widetilde{\nabla}\tilde{P} \cdot \mathbf{n}\Big|_{\tilde{r}=1} = -\gamma \sqrt{\frac{\omega_h}{\tilde{f}\tilde{P}}} \tag{21}$$

The behaviour of the system is described as a function of the two characteristic groups introduced in Eqs(18) and (20): α and γ. The dimensionless formulation expressed by Eqs(14) through (21) is henceforth referred to as “fully-coupled model” (FCM). When membrane permeability is low, the rate of recovery may not be significantly affected by the radial velocity component. In many cases of practical interest the macroscopic quantities, rather than the exact velocity profiles, need to be known. In certain conditions, such quantities may be evaluated through the use of a simpler model, in which the radial component of velocity is neglected. Furthermore, if $\tilde{\mathrm{f}}$ is considered constant and equal to its value at the inlet of the reactor, the fluid-dynamic problem becomes one-dimensional, whereas and mass transport is described by convection in the axial direction only and diffusion in both the radial and axial directions. The two problems therefore become fully uncoupled and the continuity and mass balance equations become:

$$\tilde{f}\frac{\partial}{\partial \tilde{z}}\left(\frac{\tilde{P}\partial \tilde{P}}{\partial \tilde{z}}\right) = 0 \tag{22}$$

$$\tilde{f}\nabla \cdot \left(\tilde{P}\omega_h \widetilde{\nabla}\tilde{P} - \frac{1}{Pe}\tilde{P}\widetilde{\mathbb{D}} \cdot \widetilde{\nabla}\omega_h\right) = 0 \tag{23}$$

The boundary conditions are the same as those reported in Eqs(17) and (22), whereas the pressure condition in correspondence of the membrane becomes:

$$\widetilde{\nabla}\tilde{P} \cdot \mathbf{n}\Big|_{\tilde{r}=1} = 0 \tag{24}$$

In what follows, this simplified model is referred to as “fully-uncoupled model” (FUM).

2.4 Results and discussion

Model simulations have been carried out in a wide range of parameters using the finite elements solver COMSOL Multiphysics. The number of mesh elements has been increased until no difference in the solutions obtained with a finer mesh was observed. This resulted in a problem in the order of five hundred thousand degrees of freedom. Computations times remained below one hour per run on a parallel six-processor machine regardless of parameters adopted for the specific simulation run.

The main results are shown in Figures 1-3. In these Figures all of the variables are reported in their dimensionless form. Figure 1(a) shows the dimensionless permeate flow rate evaluated with the complete model, for *Pe = 10* and two different values of *γ* (1 and 10) as a function of the operating pressure, defined by *α*. The continuous lines have been drawn as reference and their slopes are equal to 0.5 and 1.The slope of the curves changes with decreasing permeability, going from 1 to 0.5 as *γ* decreases. This suggests a transition between a condition in which permeation is controlled by mass transport within the packed bed, to one in which permeation through the membrane is the rate-limiting process. Figure 1(b) shows a comparison between the values of recovery obtained with the two different models, as a function of *γ* for two different values of *α* and *Pe=10*. Recovery is defined as the ratio between the flow rates of the permeating component across the membrane and at the inlet of the reactor. It is evident that the simplified model underestimates the recovery by about 20% when high values of *γ* are considered.

In Figures 2(a) and 2(b) a comparison between radial concentration profiles obtained with the two models is reported (points: FCM, continuous line: FUM). The curves refer to different axial positions (upper curve: $\tilde{z} = 2$,

lower curve: $\tilde{z} = 10$), evaluated at α=5x10^3, *Pe*=10, and two values of γ (1 and 10). In the first case, the profiles obtained are very similar and the low radial gradient indicates that that membrane permeability is controlling. For the higher value of γ the profiles obtained with the two models present significant differences, particularly at increasing distances from the membrane. It is reasonable to expect that this discrepancy may become even more important in non-isothermal conditions or when chemical reactions are present. The high radial concentration gradient also indicates that in the situation depicted the process is controlled by mass transfer within the packed bed.

In Figures 3(a) and 3(b) the radial dimensionless velocity profiles in different axial positions (uppermost curve: $\tilde{z} = 10$, lowermost curve: $\tilde{z} = 0.2$) for two different values of *Pe* are shown. In both cases, the value of the axial component of dimensionless velocity varies by less than 2% throughout the reactor and is of the order of 1, having chosen the inlet velocity as the characteristic quantity for the dimensionless formulation. It may be seen that when the characteristic time of dispersion is high compared to that of convection, the radial component of velocity may reach a value up to 12% of the axial component. Note that radial velocity is negative because it is directed towards the inner radius.

a) b)

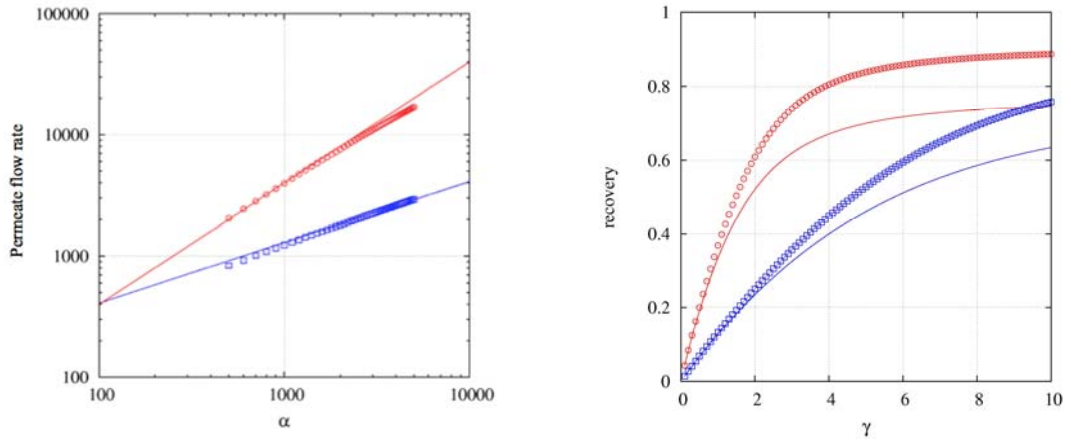

Figure 1: (a) Permeate flow rate evaluated with the FCM as a function of α for γ = 1 (lower) and 10 (upper); (b) Recovery evaluated as a function of γ for α=5x10^2 (lower) and 5x10^3 (upper) – comparison between FUM (continuous) and FCM (dotted)

a) b)

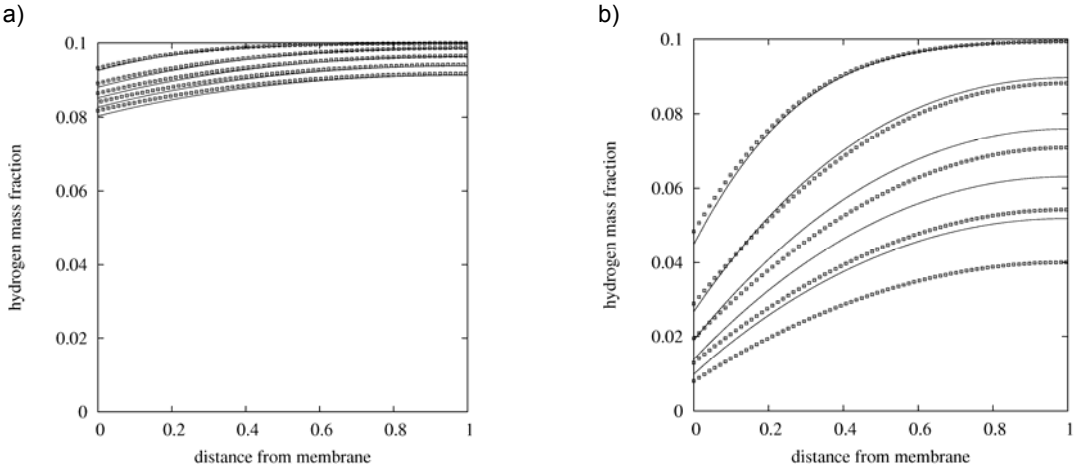

Figure 2: Radial concentration profiles evaluated with the FCM (points) and FUM (continuous line) for different axial positions. Results have been obtained with α=5x10^3, Pe=10, and γ (a) 1 and (b) 10

a) b)

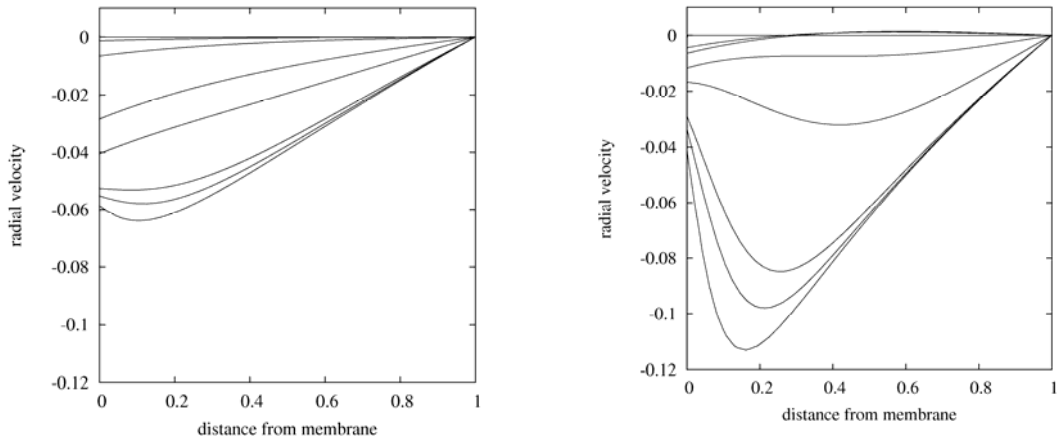

Figure 3: Radial dimensionless velocity profiles evaluated with the FCM for α=5x10², γ=10, Pe (a) 1 and (b) 10

3. Conclusions

The object of this work is to investigate the effect of different modeling approaches for predicting the performance of a membrane gas separation module presenting infinite selectivity towards one of the components. A packed-bed, co-axial cylinder geometry, where the membrane is supported onto the inner cylinder is considered. Results stemming from a detailed model, where full coupling between mass and momentum transport is enforced, are compared and contrasted to those obtained through a simplified approach, where the influence of the mass leakage through the membrane is neglected as regards the solution of the fluid dynamic problem. Significant differences are observed between model predictions both in terms of overall separator performance and qualitative structure of the concentration profiles. It is found that separation efficiency is always under-predicted when the coupling between mass and momentum transport is neglected. This finding is consistent with the observation that the fully coupled solution displays a radial velocity profile always directed towards the membrane which provides an independent transport mechanism superimposed to radial (effective) dispersion.

Acknowledgements

This work has been conducted within the framework of the CoMETHy (Compact Multifuel-Energy to Hydrogen converter) project, funded by the European Commission under the Fuel Cells and Hydrogen Joint Undertaking (GA No. 279075).

References

Giaconia, A., Turchetti, L., Monteleone, G., Morico, B., Iaquaniello, G., Shabtai, K., Sheintuch, M., Boettge, D., Adler, J., Palma, V., Voutetakis, S., Lemonidou, A., Annesini, M.C., den Exter, M., Balzer, H., 2013, Development of a solar-powered, fuel-flexible compact steam reformer: the CoMETHy Project, Chemical Engineering Transactions, 35, 433-438

Godini, H.R., Xiao, S., Kim, M., Holst, N., Jaso, S., Gorke, O., Steinbach, J., Wozny, G., 2014, Experimental and model-based analysis of membrane reactor performance for methane oxidative coupling: effect of radial heat and mass transfer, Journal of Industrial and Engineering Chemistry, 20, 1993-2202

Jin, W., Gu, X., Li, S., Huang, P., Xu, N., Shi, J., 2000, Experimental and simulation study on a catalyst packed tubular dense membrane reactor for partial oxidation of methane to syngas, Chemical Engineering Science, 55, 2617-2625

Nekhamkina, O., Sheintuch, M., 2014, Effective approximations for concentration-polarization in Pd-membrane separators, Chemical Engineering Journal, 260, 835-845

Santucci, A., Annesini, M.C., Borgognoni, F., Marrelli, L., Rega, M., Tosti, S., 2011, Oxidative steam reforming of ethanol over a Pt/Al_2O_3 catalyst in a Pd-based membrane reactor, International Journal of Hydrogen Energy, 36, 1503-1511

Ward T.L., Dao, T., 1999, Model of hydrogen permeation behaviour in palladium membranes, Journal of Membrane Science, 153, 211-231